

Guiding LLM-Based Human Mobility Simulation with Mobility Measures from Shared Data

Hua Yan

Lehigh University

Bethlehem, USA

huy222@lehigh.edu

Heng Tan

Lehigh University

Bethlehem, USA

het221@lehigh.edu

Yu Yang

Lehigh University

Bethlehem, USA

yuyang@lehigh.edu

Abstract

Large-scale human mobility simulation is critical for many science domains such as urban science, epidemiology, and transportation analysis. Recent works treat large language models (LLMs) as human agents to simulate realistic mobility trajectories by modeling individual-level cognitive processes. However, these approaches generate individual mobility trajectories independently, without any population-level coordination mechanism, and thus fail to capture the emergence of collective behaviors. To address this issue, we design M2LSimu, a mobility measures-guided multi-prompt adjustment framework that leverages mobility measures derived from shared data as guidance to refine individual-level prompts for realistic mobility generation. Our framework applies coarse-grained adjustment strategies guided by mobility measures, progressively enabling fine-grained individual-level adaptation while satisfying multiple population-level mobility objectives under a limited budget. Experiments show that M2LSimu significantly outperforms state-of-the-art LLM-based methods on two public datasets.

Keywords

Human mobility simulation; Large language model

1 Introduction

Understanding human mobility is essential for many science domains such as urban science [34, 35], epidemiology [7, 9], and transportation analysis [19, 30]. Large-scale human mobility data are usually obtained from two channels. Travel surveys record individual trips, but they are conducted infrequently and are costly, which limits their scalability [20, 31]. Sensor-based tracking methods, such as mobile-phone traces or Bluetooth beacons, provide high temporal coverage but rely on device penetration and raise significant privacy concerns [15]. Both channels struggle to scale to millions of individuals while preserving privacy.

Recent studies [1, 6, 13, 14, 16, 17, 22, 24] guide large language models (LLMs) to generate synthetic human mobility trajectories in a zero-shot way. Compared to other researches [8, 21, 42] that train a mobility/trajectory model based on real-world human mobility data, LLM-based methods enable large-scale data generation while preserving individual privacy. These methods model the LLM as a human agent, prompting it to perform step-by-step reasoning over mobility intentions based on a given user profile, and then generate trajectories accordingly. They focus on making each agent's behavior more human-like by modeling individual-level cognitive processes such as intention and reflection. However, they generate each individual's trajectory independently, without any population-level coordination mechanism, thereby failing to

capture the emergence of collective behaviors such as mobility scaling laws [3]. As demonstrated by our study (details in Section 2.1), existing simulation methods cannot fully reproduce population-level mobility behavior pattern observed in real-world data. In this work, we aim to *develop a LLM-based mobility simulation framework that preserves realistic individual behaviors while also matching population-level mobility patterns observed in real-world data*.

Prior research in social physics shows that human mobility exhibits stable and reproducible scaling laws at the population level [3, 28]. These scaling laws are typically manifested through observable mobility measures (e.g., travel distance and radius of gyration), which are typically accessible in the public shared mobility datasets, even at very coarse spatial or temporal resolution. We argue that these mobility measures can serve as population-level guidance for individual trajectory generation. For example, the radius of gyration [10] quantifies the spatial range of individual mobility, and has been shown to follow a truncated power-law distribution. By comparing the distributions observed in real-world data with those generated by simulation, we can identify differences, such as fewer short-distance trips (around 1 km) and more very long-distance trips (beyond 200 km) in the simulated trajectories. These differences provide diagnostic signals, indicating which types of individuals are not adequately captured by the generative process. Based on this analysis, we can tailor individual-level prompts by incorporating explicit behavioral constraints and persona descriptions, so that different individuals are guided by distinct prompts rather than sharing a single prompt that varies only in profile information. This allows us to capture population heterogeneity and thus reproduce realistic mobility behaviors.

In this work, we leverage mobility measures as guidance to adjust individual-level prompts in order to generate more realistic population-level mobility behaviors, as shown in Figure 1. These mobility measures are traditionally derived from detailed real-world trajectory data; moreover, we find that they are largely preserved even in coarse-grained shared datasets (details in Section 2.3). This observation is consistent with emerging data-sharing practices (e.g., sharing coarse-grained trajectories [37], validated simulation results [40], or aggregated statistics [10]) and suggests that our approach can operate effectively under limited data access, improving both generalizability and practical deployability.

While mobility measures provide useful guiding signals at the population level, several challenges still remain: (i) Because mobility measures characterize different aspects (e.g., spatial and temporal) of population behavior rather than individual behavior, it remains unclear which specific individuals should be adjusted or whether one or multiple aspects of their behavior need to be modified. For example, if a simulation produces too few short-distance trips and

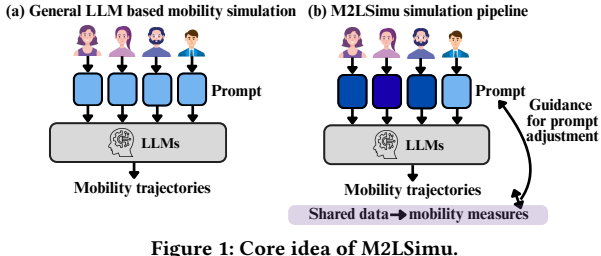


Figure 1: Core idea of M2LSimu.

insufficient activity around midday or at night, this does not imply that all adjusted individuals should both travel short distances and be highly active during those periods. Moreover, adjustments aimed at satisfying one mobility measure must be coordinated with other measures to avoid unintended conflicts. (ii) Each adjustment requires re-running the LLM-based simulation for multiple individuals followed by population-level evaluation, which leads to high computational costs.

To address the challenges, we view the prompt adjustment problem as a multi-objective, multi-prompt optimization task. We formulate the prompt adjustment process as a Markov Decision Process, where the state represents the current set of prompts for all individuals, and each action corresponds to a coarse-grained prompt adjustment strategy applied to a group of individuals, generated by an LLM. Although these strategies are defined at a coarse level (without targeting specific individuals), our framework operates in an iterative manner, allowing different individuals to undergo different combinations of adjustments and resulting in fine-grained individual-level adjustment that enables the coordinated satisfaction of multiple mobility-law objectives at the population level. We design a multi-objective reward function to encourage improvements along one mobility-law objective while maintaining consistency with others. To reduce the computational cost of reward evaluation, we employ Monte Carlo Tree Search to solve this optimization problem, as it progressively allocates evaluation budget to promising branches while balancing exploration and exploitation. In addition, we introduce a global action value estimator to perform coarse candidate filtering. We perform the search on a small subset of the population, and then generalize the resulting adjustments to larger groups of individuals with similar profiles.

In particular, our main contributions are as follows.

- We explore the idea of leveraging mobility measures from shared data as guidance to adjust individual prompts in order to generate realistic population-level mobility behavior.
- We design M2LSimu, a Mobility Measures-guided Multi-prompt Adjustment Framework for Large-scale LLM-based Human Mobility Simulation. Our framework utilizes coarse-level adjustment strategies based on mobility measures guidance and operates in an iterative manner. This process automatically enables fine-grained individual-level adjustment, supporting satisfaction of multiple mobility-law objectives at the population level under a limited budget.
- We conduct extensive experiments on two public datasets, and the results demonstrate that our method achieves the best performance, with improvements ranging from 11.29% to 64.08% over the best baseline across multiple metrics. In addition, we evaluate the impact of different types of shared

data on our method. The results show that mobility measures obtained from different types of shared data can effectively guide LLM-based mobility simulations. Notably, even statistical shared data, without trajectory-level information, leads to noticeable performance improvements.

2 Motivation

2.1 Limitations in reproducing scaling laws

In this section, we use two classical laws of human mobility (i.e., travel distance and visitation frequency) to show that existing simulations cannot fully reproduce population-level mobility behaviors observed in real-world data. Specifically, we select a representative human mobility simulation work, LLMob [13], and compare its results with real-world data of Beijing (details in Section 4.1).

Travel distance: travel distance characterizes the distance Δd between consecutive locations in an individual's mobility trajectory, capturing the scale of human mobility [10]. It follows a truncated power-law, $P(\Delta d) \sim (\Delta d + \Delta d_0)^{-\beta} \exp\left(-\frac{\Delta d}{\kappa}\right)$, where Δd_0 is a small offset parameter. The exponent β determines how frequently long-distance movements occur, with larger values leading to fewer long trips and smaller values leading to more long trips. The cutoff κ captures the spatial extent of individual mobility.

We compute the travel distance from both the real-world data and the simulation and visualize their complementary cumulative distribution functions (CCDFs), as shown in Figure 2. The real-world data are well described by a truncated power-law, with parameter values consistent with those reported in previous studies [10] (with $\beta \approx 1.75 \pm 0.15$ and $\kappa \approx 400$ km). In contrast, for the simulation, the estimated scaling exponent is smaller ($\beta \approx 1.22$), and is accompanied by a cutoff at around ($\kappa \approx 1039.3$ km), which is much larger than that observed in real-world data. These results show that the simulation produces too many long-distance trips and does not capture the strong decline in such trips observed in real-world data.

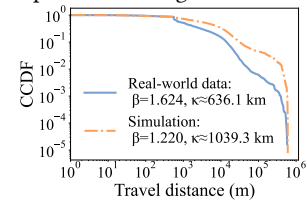


Figure 2: Travel distance distribution (Real vs. Simulation).

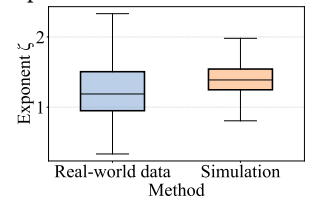


Figure 3: Visitation frequency (Real vs. Simulation).

Visitation frequency: It describes the rank-frequency relationship of an individual's visited locations. The visitation frequency f_k of the k -th most frequently visited location follows $f_k \propto k^{-\zeta}$, where $\zeta \approx 1.2 \pm 0.1$ in a prior study [28]. A larger value of ζ indicates that the individual concentrates visits on a small number of core locations, whereas a smaller ζ implies a greater tendency to explore new locations. For each user, we estimate ζ and compare the resulting distributions across users between the real-world data and the simulation, as shown in Figure 3. We observe that the simulation produces insufficient heterogeneity compared with the real-world data. In the real-world dataset, some individuals tend to explore a large number of new locations, while others repeatedly return to a small set of core places. This result indicates that the simulation fails to fully capture population-level mobility pattern.

2.2 A preliminary study on the effectiveness of mobility measures guidance

In this section, we aim to provide a preliminary validation of whether mobility measures are effective as guidance. Specifically, we focus on a single target mobility measure (i.e., radius of gyration). We first compute the radius distribution from simulated data. Next, we prompt another LLM to analyze the differences between the simulated and target radius distributions. Based on this analysis, the LLM provides coarse adjustment suggestions. We then randomly select 5% of individuals for prompt adjustment and generate new trajectories using the updated prompts. We then visualize the cumulative distribution functions (CDFs) of the radius distributions for the real-world data, the simulation, and the adjusted trajectories, as shown in Figure 4. We observe that mobility measure-guided adjustments bring the simulated trajectories closer to real-world patterns. Nevertheless, a discrepancy remains, partly because the adjustment strategy was simple. Furthermore, the challenge remains because mobility measures characterize population-level behavior across multiple dimensions (e.g., spatial and temporal), rather than capturing single-aspect behaviors at the individual level, making it unclear which specific individuals should be adjusted or whether one or multiple aspects of their behavior need to be modified.

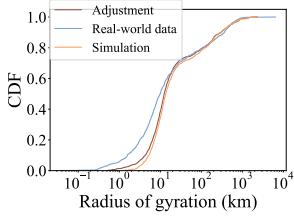


Figure 4: Comparison of radius of gyration.

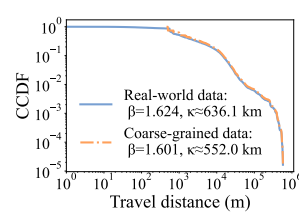


Figure 5: Travel distance (Real vs. Coarse-grained).

2.3 Preservation of human mobility scaling laws in coarse-grained data

In this section, we examine whether coarse-grained trajectories preserve the scaling laws of human mobility observed in real-world data. Following [37], we map the geographic coordinates of real-world data onto a 500 m \times 500 m spatial grid and compute all distances in the grid space. Time is discretized into intervals of length 48 to construct coarse-grained trajectories. Based on both real-world and coarse-grained data, we compare travel distance distributions, stay duration distributions, and visitation frequency from spatial, temporal, and spatial-temporal perspectives. Due to space constraints, we report only the spatial results here (i.e., Figure 5), while the remaining results are provided in the appendix. Results indicate that coarse-grained data preserves key laws.

3 Design

3.1 Problem formulation

We model the LLM as a simulator to generate human mobility trajectories. Given a prompt that consists of an individual's user profile, a task description, and additional behavioral constraints, the LLM generates a corresponding mobility trajectory. To support large-scale simulations, we generate trajectories for a population of

n individuals in parallel, where each individual is associated with a distinct prompt and produces mobility trajectories. At initialization, all individuals share the same base prompt, while personalization is achieved through differences in their user profiles.

We can adjust prompts at the individual level by incorporating explicit behavioral constraints and detailed persona descriptions based on mobility measure guidance. This allows different individuals to be guided by distinct prompts, rather than relying on a single shared prompt that differs only in profile information. This work aims to identify a set of prompts for large-scale mobility simulation to improve the realism of human mobility behaviors across multiple mobility measures. We therefore formulate prompt adjustment for human mobility simulation as a **multi-objective, multi-prompt optimization problem**. Let $\mathcal{P} = \{p^1, \dots, p^n\}$ denote the set of prompts assigned to n individuals, and let $\{Y^1, \dots, Y^n\}$ denote the corresponding trajectories generated by the LLM. Given a set of evaluation objectives $\mathcal{X}^* = \{x^{*(1)}, \dots, x^{*(D)}\}$, our goal is to find an optimal \mathcal{P} that jointly optimizes all objectives in \mathcal{X}^* .

3.2 Overview

We design M2LSimu, a multi-prompt adjustment framework for LLM-based human mobility simulation, guided by mobility measures from shared data, as shown in Figure 6. First, we use a simulation model that takes initial prompts as input to generate a set of mobility trajectories. Second, we have different types of shared data that can be used to evaluate the quality of the generated trajectories and provide different mobility measures as guidance for the generation process (details in Section 3.4). Third, in order to leverage the guidance provided by the shared data to identify an optimal set of prompts for improving simulation, we formulate the prompt adjustment process as a Markov Decision Process, where the state represents the current set of prompts for all individuals, and each action corresponds to a coarse-grained prompt adjustment strategy applied to a group of individuals, generated by an LLM. We then use Monte Carlo Tree Search to find an optimal set of prompts (details in Section 3.3 and Section 3.5). Finally, this optimized set of prompts can be used for human mobility simulation and can also be extended to larger populations based on similar profiles, thus reducing the cost of prompt adjustment (details in Section 3.6).

3.3 M2LSimu MDP formulation

We model the prompt adjustment process as a Markov Decision Process (MDP) defined by the tuple $(\mathcal{S}, \mathcal{A}, \mathcal{T}, r)$. \mathcal{S} denotes the set of states; \mathcal{A} denotes the action space; \mathcal{T} denotes the state transition; r is the reward function. We introduce $\mathcal{S}, \mathcal{A}, \mathcal{T}, r$ in detail as follows.

States \mathcal{S} : The state $s_t \in \mathcal{S}$ represents the current set of prompts assigned to a population of n individuals: $s_t = \{p_t^1, p_t^2, \dots, p_t^n\}$. At initialization, all individuals share the same base prompt, i.e., $p_0^i = p_{\text{init}}$, while personalization is achieved by different user profiles.

Action \mathcal{A} : An action $a_t \in \mathcal{A}$ corresponds to a prompt adjustment strategy generated by an LLM. The action space \mathcal{A} consists of a set of such prompt adjustment strategies. We next introduce how the actions are generated. We first select target mobility measures according to different types of shared data. Based on these targets, we then compute the corresponding metrics from the simulated trajectories. Finally, we prompt another LLM to analyze the gaps

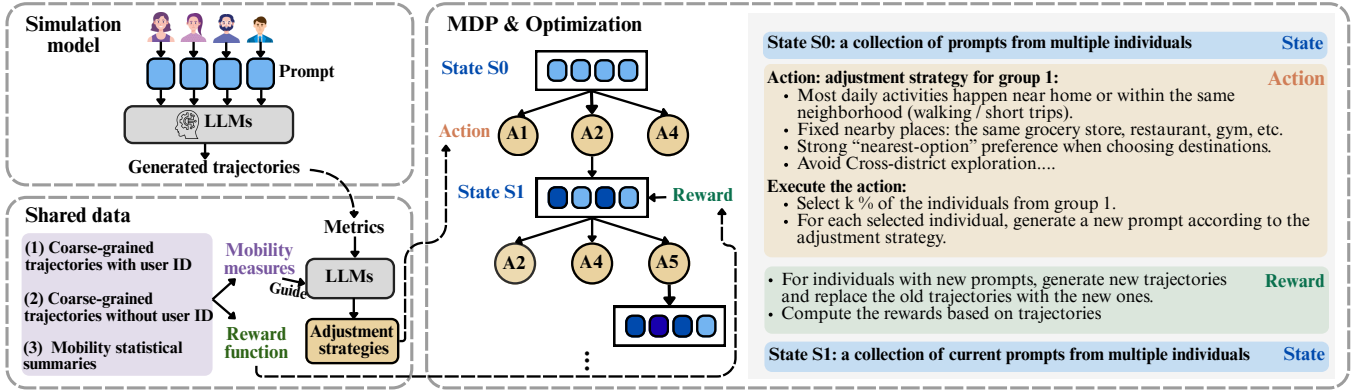


Figure 6: Framework of M2LSimu.

between a specific target measure and the corresponding simulated one. From a population-level perspective, this LLM examines the simulated data, partitions individuals into multiple groups based on their mobility behaviors, and proposes corresponding prompt adjustment strategies for each group (see an example in Figure 6). Each group-specific prompt adjustment strategy is treated as a single action. We apply the same procedure to all target measures (e.g., spatial and temporal) and aggregate the resulting actions to form the action set. Different types of shared data mainly differ in the form of target measures (e.g., distributional vectors or scalar parameters) and the information available to the LLM; detailed formulations are provided in Section 3.4.

Transition \mathcal{T} : The transition function $\mathcal{T} : \mathcal{S} \times \mathcal{A} \rightarrow \mathcal{S}$ defines how the framework transitions to the next state by applying a selected adjustment strategy to the current prompt set. Given a group-specific action a_t , we select $k\%$ of the individuals from the corresponding group. For each selected individual, we prompt another LLM to generate an updated prompt based on the current prompt s_t and the associated prompt adjustment a_t . We update only the prompts of the selected individuals, while all other prompts remain unchanged from s_t . The updated set of prompts defines the next state $s_{t+1} = \mathcal{T}(s_t, a_t)$.

Reward r : The reward function r measures the quality of the simulation at each step. To balance multiple mobility measures and avoid large drops in any single metric, we define the reward as the geometric mean of normalized quality scores [12]. Let $\mathbf{x}_t = (x_t^{(1)}, \dots, x_t^{(D)})$ denote the vector of mobility measures observed at step t , where $x_t^{(i)}$ represents the i -th mobility measure. Depending on the type of shared data, $x_t^{(i)}$ may be either a scalar or a vector. Let \mathbf{x}^* denote the corresponding target vector. For each mobility measure i , we define a function $g(x_t^{(i)}, x^{*(i)})$ that measures the distance to the target one, whose specific definition depends on the type of shared data (details in Section 3.4). We aggregate the multi-dimensional qualities using a geometric mean, which encourages balanced improvements across dimensions and penalizes actions that improve dimensions at the expense of others: $R(t) = \left(\prod_{i=1}^D (g(x_t^{(i)}, x^{*(i)}) + \epsilon) \right)^{\frac{1}{D}}$, where $\epsilon > 0$ is a small constant introduced for numerical stability. The immediate reward is defined as the improvement of the aggregated quality between consecutive steps: $r_t = R(t) - R(t+1)$.

3.4 Mobility measures from different types of shared data

We consider three typical types of shared data, each providing different mobility measures for guidance. All such measures are compatible with our framework; the key difference lies in how they influence action generation and the design of the reward function.

(1) Mobility measures from shared data: coarse-grained trajectories with user IDs. This type of shared data [37] is available at the user level, where each trajectory is linked to a unique but anonymous user ID. We select several mobility measures as the target to guide prompt adjustment. In the following, we describe the selected target measures and discuss the reasons for choosing them. We select the radius of gyration, stay duration, and visitation frequency as target measures, representing the spatial, temporal, and spatial-temporal dimensions of the mobility measures, respectively. We choose these measures because they are representative of the three dimensions and have been widely studied in human mobility research, where power-law scaling has often been reported [10, 28]. In addition, these measures can be computed at the user level, enabling analysis of differences across population groups.

For action generation, we provide the LLM with the CCDF distributions of the radius of gyration and stay duration, as well as the distribution of user-specific ζ in visitation frequency, for analysis. For the reward function: we define the function $g(x_t^{(i)}, x^{*(i)})$ measuring the discrepancy between the simulated mobility metric $x_t^{(i)}$ and its target value $x^{*(i)}$, where $x_t^{(i)}$ is a vector. This function consists of two components: a scale-sensitive deviation from the target and a distribution discrepancy. For the first component, we compute the 1-Wasserstein distance in log space, which is defined as $\mathcal{L}_{W1}(x_t^{(i)}, x^{*(i)}) = W_1(\log(x_t^{(i)} + \epsilon), \log(x^{*(i)} + \epsilon))$, where ϵ is a small constant to ensure numerical stability. For the second component, we measure distance between the two CCDFs: $\mathcal{L}_{L1}(x_t^{(i)}, x^{*(i)}) = \int |\hat{C}_t^{(i)}(z) - \hat{C}_*^{(i)}(z)| dz$, where $\hat{C}_t^{(i)}$ and $\hat{C}_*^{(i)}$ denote the CCDFs of $x_t^{(i)}$ and $x^{*(i)}$. Finally, the function $g_i(x_t^{(i)}, x^{*(i)})$ is defined as $g(x_t^{(i)}, x^{*(i)}) = \mathcal{L}_{W1}(x_t^{(i)}, x^{*(i)}) + \mu \mathcal{L}_{L1}(x_t^{(i)}, x^{*(i)})$, where μ is a weighting coefficient.

(2) Mobility measures from shared data: coarse-grained trajectories without user IDs. This type of shared data [40] is not available at the user level and consists only of independent

trajectories. Consequently, mobility measures that rely on user-level information (e.g., radius of gyration) or long-term mobility history (e.g., revisit probabilities) cannot be computed. For the target measures, we select travel distance and stay duration, which are computed at the trajectory level and represent the spatial and temporal dimensions, respectively. The travel distance is adopted as the spatial metric, as it reflects individual mobility decisions and directly influences higher-level spatial mobility metrics, such as the radius of gyration and the travel range.

For action generation, we provide the LLM with the CCDF distributions of the travel distance and stay duration, as well as the distribution of user-specific ζ in visitation frequency, for analysis. For the reward function, we use the same distance function as in the first type of shared data setting.

(3) Mobility measures from shared data: mobility statistical summaries This type of shared data includes only reported statistical summaries, without explicit trajectory information, e.g., parameters exponent β describing travel distance distributions from prior studies [10]. Such data provide only coarse-grained guidance for mobility simulations. For example, by comparing the exponent and cutoff parameters of travel distance distributions between real-world and simulated data, we can infer whether certain population groups are potentially overrepresented or underrepresented. Following the first type of shared data, we select the radius of gyration, stay duration, and visitation frequency as target metrics.

For action generation, the LLM is provided with statistical summaries, including the exponent and cutoff parameters of the travel distance and stay duration distributions, as well as the total ζ associated with visitation frequency. For the reward function: as the mobility measure $x_t^{(i)}$ is a scalar, we define the function measuring the distance to the target value $x^{*(i)}$ as $g(x_t^{(i)}, x^{*(i)}) = \frac{|x_t^{(i)} - x^{*(i)}|}{x^{*(i)}}$.

3.5 Optimization

We apply Monte Carlo Tree Search (MCTS) within this MDP framework to efficiently explore the action space under a limited evaluation budget [33]. In our formulation, each node represents a state and each edge corresponds to an action, while a state-action value function estimates the expected cumulative reward of applying an action at a given state. The search tree is progressively constructed by iteratively performing four MCTS operations: selection, expansion, simulation, and back-propagation.

Selection. At each iteration, the algorithm starts from the root state s_0 and recursively selects actions among the existing child nodes in the search tree until a leaf node is reached. The goal of this step is to focus the search on promising actions while still exploring less frequently tried ones. At a state s , the action is selected from the set of actions that have already been expanded in the search tree. For each such action a , an Upper Confidence Bounds applied to Trees (UCT) score is computed as: $UCT(s, a) = Q(s, a) + c \sqrt{\frac{\ln(N(s)+1)}{N(s,a)+1}}$, where $Q(s, a)$ denotes the mean reward of choosing action a at state s and c is the exploration constant that controls the trade-off between exploration and exploitation. $N(s)$ is the visit count of state s , and $N(s, a)$ is the visit count of the corresponding state-action pair. The action selected is given by $a^* = \arg \max_{a \in C} UCT(s, a)$.

Expansion. The expansion step enlarges the search tree by introducing new child nodes from the leaf node selected in the

selection phase. Given a leaf node state s , we first use a global filtering policy to generate candidate action set C . This step allows our method to concentrate its computational budget on a small number of globally promising actions. For each action $a \in A$, we maintain a global average reward $Q_g(a)$ and a usage count $N_g(a)$. A global Upper Confidence Bound (UCB) score is computed as

$$UCB_g(a) = Q_g(a) + c_g \sqrt{\frac{\ln(\sum_{b \in A} N_g(b) + 1)}{N_g(a) + 1}}, \quad (1)$$

where c_g is a constant controlling the exploration and exploitation trade-off. The top n actions with the highest UCB_g scores are selected to form a candidate set C . For each candidate action $a \in C$, we can obtain its next by the state transition function, and an immediate reward $r(s, a)$ by the reward function. Among the evaluated candidates, the action with the highest immediate reward is selected, $a^* = \arg \max_{a \in C} r(s, a)$, and the corresponding state s_{a^*} is added to the search tree as a new child node and forwarded to the subsequent simulation stage.

Simulation. The simulation phase estimates long-term returns by performing a forward rollout starting from the newly expanded state. Given the initial state s' , the algorithm iteratively applies a rollout policy, while no additional tree nodes are created during simulation. At each rollout step, we first generate a candidate action set C using the global filtering policy. For each $a \in C$, we obtain the resulting state $s_a = \mathcal{T}(s, a)$ and the immediate reward $r(s, a)$ through the transition function and the reward function. We then select the action with the highest immediate reward to advance the rollout. The rollout terminates when a predefined stopping criterion is met, such as reaching a maximum rollout depth.

Back-propagation. After a rollout trajectory is completed, the observed rewards are propagated backward along the trajectory to update the value estimates of the state-action pairs on the search tree that were encountered during the rollout. Unlike incremental one-step updates, we estimate the action value based on the average cumulative rewards of all future trajectories originating from the same state-action pair. Formally, let (s_t, a_t) denote a state-action pair on the search tree that is encountered along a rollout trajectory, and let M be the total number of rollouts that have passed through (s_t, a_t) . For the j -th rollout, denote by $\text{traj}_j(s_t, a_t)$ the sub-trajectory starting from (s_t, a_t) until termination. $Q(s_t, a_t)$ is defined as $Q(s_t, a_t) = \frac{1}{M} \sum_{j=1}^M \left(\sum_{(s', a') \in \text{traj}_j(s_t, a_t)} r(s', a') \right)$, where the inner summation corresponds to the cumulative reward collected along the future trajectory following (s_t, a_t) .

3.6 Using the optimal prompt set

After identifying the optimal prompts, we can directly use the updated prompt set to generate new mobility trajectories. These prompts can also be scaled to larger populations. To reduce the computational cost of searching for the optimal prompt set, we first randomly sample a subset of users and perform prompt optimization on this group. Once the optimized prompts are obtained, we scale them to the full population. Specifically, for each adjusted prompt, we assign it to the m most similar users in the full population based on profile similarity, where m is determined by the population size ratio between the subset and the full population.

4 Evaluation

4.1 Dataset description

We use two public mobility datasets. One dataset is collected in Beijing, China, covering the period from October 1, 2019 to December 31, 2019 [24]. The dataset contains mobility trajectories and user profile information (e.g., age, gender, and occupation), collected via a social networking platform. The other dataset is a global simulation dataset that has been validated under scaling laws of human mobility [40]. All trajectory points are discretized into spatial grids of 1000×1000 meters, and time is discretized into 48 time slots per day. The dataset does not contain user identifiers. We select one city (New York City) from this dataset, which includes over 100,000 trajectories. In our simulation setting, user profile data are required as inputs, and mobility trajectories are used for validation. We select these two datasets because they satisfy both requirements and cover different countries and cities. Some other publicly available datasets are not suitable for our setting. For example, datasets [37] do not release city-level information, making it impossible to construct individual-level profiles. In addition, POI check-in datasets are less appropriate, as their sparse records do not align well with the daily mobility patterns considered in our simulations.

For the Beijing dataset, we select 1,200 individuals with approximately one month of data from the real-world dataset as the ground truth. All baseline methods and our approach leverage user profiles and an LLM to generate one-month synthetic human mobility trajectories. For the New York dataset, we use the entire dataset as the ground truth. We simulate user profiles based on U.S. Census demographics [4], and employ an LLM to generate two-week synthetic human mobility trajectories.

4.2 Evaluation setup

4.2.1 Implementation. For our method M2LSimu, we use the first type of shared data as mobility measure guidance. The LLM we use is GPT-5.2. Our initial simulation model is based on [1], but differs in that the original method uses a gravity model to generate locations, whereas we directly leverage an LLM to generate locations. For the transition function, we set $k = 10$. For the reward function, we set $\mu = 0.5$. In the MCTS search, the maximum tree depth is set to 10, three candidate nodes are selected at each step, and a total of 50 simulations are performed. The exploration constants are set to $c = 1.4$ and $c_g = 1.0$. To determine profile similarity, we employ the pre-trained language model [29]. In our work, we select 30% of users to search for the optimal prompt set and then extend the resulting prompts to the full population.

4.2.2 Baselines. We compare our method with LLM-based human mobility simulation baselines: **CoPB** [24] is a mobility simulation framework that guides LLMs through structured reasoning stages to generate realistic mobility intentions. **Urban-Mobility-LLM (UML)** [1] is a method that synthesizes travel survey data by prompting LLMs to generate individual mobility patterns. **LL-Mob** [13] is an LLM-based agent framework for personal mobility generation, combining self-consistency and retrieval strategies. **CitySim** [2] leverages LLM-powered agents with personas, memory, and long-term goals to simulate realistic human behavior.

We also conduct comparisons with several variants of the model: (1) We consider two additional types of shared data as guidance through mobility measures, namely **M2LSimu with the second Shared Data (w SD2)** and **M2LSimu with the third Shared Data (w SD3)**. (2) **M2LSimu with Two Aspect mobility measures as guidance (w TA)**. In this setting, we only use mobility measures from spatial and temporal as guidance. (3) **M2LSimu without Prompt Adjustment (w/o PA)**. In this setting, we remove the prompt adjustment part. (4) **M2LSimu without Extension (w/o E)**. In this setting, we perform the search on the full dataset.

4.2.3 Metric. Following existing simulation work [13, 24], we evaluate our model using three aspects metrics. To assess the similarity between the simulation and real-world data, we compute the Jensen–Shannon divergence (JSD) between their distributions for each metric. It is worth noting that the evaluation metrics include the mobility measures used as guidance. While we report results for all metrics, performance improvements are evaluated only on metrics excluding the guidance measures.

Spatial aspect: (1) Radius of gyration: quantifies the spatial extent of an individual's mobility. We compute the radius of gyration as the root mean square distance of visited locations from the trajectory centroid. (2) Travel distance: defined as the geographical distance between consecutive locations in a trajectory. (3) Origin–destination similarity (OdSim): quantifies the similarity between generated and real trajectories in terms of OD travel patterns. It is computed by comparing the normalized frequency distributions of OD pairs using JSD.

Temporal aspect: (1) Stay duration: measures how long individuals remain at each visited location. We compute the duration distribution from the time intervals between consecutive movements. (2) Circadian rhythm: This metric [23] captures the circadian rhythm of human mobility intensity over a 24-hour period. We quantify it by aggregating trips into hourly bins.

Spatial-temporal aspect: (1) Visitation frequency. This metric [28] describes the rank-frequency relationship of an individual's visited locations. The detailed definition is in Section 2. (2) Exploration: This metric [28] characterizes how the number of distinct locations grows with the total number of visits. Let H denote the number of stays and $N_{\text{new}}(H)$ the cumulative number of unique locations. Exploration follows a sublinear power-law, $N_{\text{new}}(H) \sim H^\alpha$, where α is the exploration exponent. We estimate α for each user and compare its distribution between real and simulated data. (3) Preferential return: Following [28], we characterize preferential return as the tendency to revisit previously visited locations with probability proportional to their past visitation frequency. Let $n_i(t)$ denote the number of visits to location i prior to time t . Following the original linear assumption ($P \propto n_i$), where P denotes the probability of returning to location i , we generalize the model by fitting $P \propto n_i^\gamma$, where $\gamma = 1$ corresponds to linear preferential return. As the evaluation metric, we report the mean absolute error (MAE) between the estimated exponent γ from simulated and real data.

4.3 Overall performance

4.3.1 Overall performance on Beijing dataset. We compare our method M2LSimu with other baseline methods, as shown in the Table 1. For our method M2LSimu, we use the first type of shared

Table 1: Overall Performance on Beijing dataset. Bold scores are for the best values. The gray-shaded parts indicate the metrics used for evaluation under the specific shared data setting.

Method	Spatial			Temporal		Spatial-temporal		
	Radius	Distance	OdSim	Duration	Circadian	Visitation frequency	Exploration	Return
CoPB	0.0618	0.0194	0.2231	0.0255	0.1072	0.1829	0.1738	0.1063
UML	0.0351	0.0142	0.2399	0.0172	0.0770	0.2087	0.2483	0.0837
LLMob	0.0631	0.0289	0.1497	0.0199	0.0735	0.1256	0.1275	0.2214
CitySim	0.0344	0.0163	0.2524	0.0181	0.1513	0.2792	0.2218	0.2344
M2LSimu w SD2	0.0299	0.0056	0.1301	0.0156	0.0712	0.1643	0.1424	0.0764
M2LSimu w SD3	0.0312	0.0061	0.1306	0.0158	0.0718	0.1096	0.0882	0.0347
M2LSimu	0.0270	0.0051	0.1271	0.0152	0.0652	0.1000	0.0667	0.0303

Table 2: Overall Performance on NYC dataset. Bold scores are for the best values. The gray-shaded parts are the metrics used for evaluation under the specific shared data setting.

method	Spatial		Temporal	
	Distance	OdSim	Duration	Circadian
CoPB	0.0840	0.1453	0.1566	0.1272
UML	0.0763	0.2190	0.1255	0.1169
LLMob	0.0932	0.1472	0.1031	0.1270
CitySim	0.0865	0.1612	0.1429	0.2063
M2LSimu w SD2	0.0559	0.1283	0.0465	0.0881
M2LSimu w SD3	0.0535	0.1286	0.0572	0.1039

data to provide guidance. As guidance, we chose mobility measures from three aspects: radius, stay duration, and visitation frequency, corresponding to the spatial, temporal, and spatio-temporal perspectives respectively. The other metrics were used for validation, shown in gray. From the Table, we can see that our method outperforms all other baselines, achieving at least an improvement of 64.08% in travel distance, 15.09% in odSim, 11.29% in circadian, 47.69% in exploration, and 63.80% in return. This demonstrates that using mobility measures as guidance can effectively guide individual generation, and produce better collective behavioral patterns.

4.3.2 Overall performance on NYC dataset. For the New York City dataset, we only consider the latter two types of shared data as guidance, since the dataset does not provide user-level trajectories. In addition, we evaluate only spatial and temporal metrics, as the absence of user IDs prevents the computation of spatial-temporal metrics. As guidance, we chose radius and stay duration as mobility measures, corresponding to the spatial and temporal perspectives respectively. The other metrics were used for validation, shown in gray. We compare our method M2LSimu with other baseline methods, as shown in Table 2. From the Table, we can see that our method outperforms all other baselines, achieving at least an improvement of 11.70% in OdSim, 24.63% in Circadian.

4.4 Performance across shared data types

In this section, we study how different types of shared data affect prompt adjustment for simulation, and whether good performance can still be achieved using only statistical summaries.

4.4.1 Performance across shared data types on Beijing dataset.

For the Beijing dataset, we consider three types of shared data and select metrics from three perspectives: spatial, temporal, and

spatio-temporal. We compare our method M2LSimu with variants, as shown in the Table 1. Due to data type limitations, different shared data settings use different mobility measures as guidance. Therefore, we use the metrics not included as guidance for evaluation, as shown in gray. We can observe that using the first type of shared data (i.e., M2LSimu) achieves the best performance, because each mobility measure is computed at the user level, allowing more precise identification of issues across different individuals. The performance of using the third type of shared data (i.e., M2LSimu w SD3) slightly decreases, since having only mobility statistical summaries can provide only a coarse direction for improvement. Nevertheless, the overall performance of M2LSimu w SD3 remains good and outperforms all baselines.

4.4.2 Performance across shared data types on NYC dataset.

For the New York City dataset, we consider two types of shared data and select metrics from spatial and temporal aspects. We compare two variants of our method M2LSimu, as shown in Table 2. Similarly to the Beijing dataset, we use the metrics not included as the guidance for evaluation, as shown in gray. Overall, using the second shared data (i.e., M2LSimu w SD2) performs slightly better than using the third shared data (i.e., M2LSimu w SD3), because M2LSimu w SD2 provides more fine-grained rewards. Similar to the findings in the Beijing dataset, even when M2LSimu w SD3 uses mobility statistical summaries as the guidance, performance remains good and outperforms all baselines.

4.5 Ablation study

To evaluate whether guidance from a single mobility measure dimension can improve performance in other dimensions, we use spatial and temporal mobility measures as guidance and assess improvements in the spatial-temporal dimension (i.e., M2LSimu w TA) on the Beijing dataset. We compare M2LSimu, M2LSimu without prompt adjustment (i.e., M2LSimu w/o PA), and M2LSimu w TA, as illustrated in the figure. From the Figure 7, we observe that M2LSimu w TA achieves performance comparable to M2LSimu in both the spatial and temporal dimensions. However, in the spatial-temporal dimension, it performs worse than M2LSimu. Nevertheless, relative to M2LSimu w/o PA, M2LSimu w TA shows clear improvement. These results suggest that using spatial and temporal mobility measures as guidance can contribute to improvements in the spatial-temporal dimension.

To validate whether the optimal prompt set obtained from a small subset of the population can generalize to a larger population,

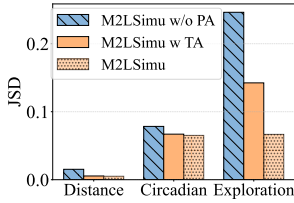


Figure 7: Effect of spatial and temporal guidance on spatial-temporal performance.

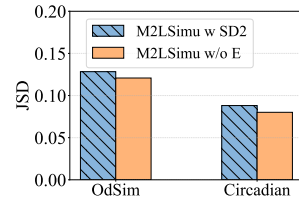


Figure 8: Performance of optimal prompt scaling from a subset to the full population.

we conduct an experiment using the NYC dataset. We choose this dataset since it has fewer users and trajectories, resulting in lower computational cost for full-dataset search. Specifically, we perform the search on the full dataset (i.e., M2LSimu w E), and compare the results with M2LSimu w SD2. As shown in the Figure 8, the results are comparable, indicating that the optimal prompt set identified from a small subset can be generalized to a larger population.

We further assess whether prompt adjustment improves the realism of simulated mobility behaviors through scaling-law-based analysis (see Appendix for details).

4.6 Overhead analysis

In this section, we analyze the additional overhead of prompt adjustment by counting LLM calls. For the Beijing dataset, generating one month of trajectories for 1,200 individuals requires approximately 36,000 LLM calls. For prompt adjustment, we randomly select 30% of individuals to search for optimal strategies, and the optimized prompt is then applied to the entire population. During the prompt search process, this results in approximately 39,520 additional LLM calls, roughly equivalent to one extra simulation.

5 Limitations and ethical considerations

Lessons learned: Based on the results of our paper, we summarize the following lessons learned: (1) Mobility measurements obtained from different types of shared data can effectively guide LLM-based mobility simulations, as shown in Table 1 and Table 2. Even statistical information without any trajectories leads to noticeable performance improvements. (2) Our framework incorporates multi-dimensional mobility measurements as guidance, enabling improvements that extend beyond targeted aspects and enhance the overall mobility simulation, as shown in Table 1 and Figure 7. (3) Our framework enables identifying optimal prompt combinations from a small subset of individuals and generalizing them to a larger population, reducing search overhead, as shown in Figure 8.

Limitation: Despite its effectiveness, our framework has several limitations. Our framework introduces additional computational overhead in mobility simulation, particularly at large scales, although this cost is partially mitigated by our method. Our evaluation is currently limited to two cities and extending validation to more diverse urban environments remains future work.

Ethics and privacy: This work focuses on population-level mobility simulation rather than individual tracking or prediction. Our framework uses user profiles as inputs, which are derived from census statistics or publicly available data. All information is highly anonymized and represented at a coarse-grained level, preventing identification of individuals. Mobility measures are obtained

from publicly shared data and do not involve privacy-sensitive information. While LLM-based simulations may introduce biases or unrealistic behaviors, our framework uses mobility measures to guide individual generation for improving realism.

6 Related work

LLM-based human mobility simulation. Existing works explored using LLMs for human mobility simulation by leveraging their knowledge and human-like reasoning capabilities. The advantage of these approaches is that they do not require large-scale real-world mobility data for training. These works [1, 6, 13, 14, 16–18, 22, 24] guide LLMs to simulate human-like mobility intention reasoning step by step and then produce realistic mobility activity sequences. For example, CoPB [24] is an intention- and planning-based framework that enables LLMs to generate human mobility trajectories through step-by-step reasoning. Although these works produce realistic outputs, the reliance on LLMs makes the simulation expensive. This work [13] designs a LLM-based agent framework for personal mobility generation, combining self-consistency and retrieval strategies to align language models with real-world human activity for accurate and interpretable mobility simulation.

However, they generate each individual's trajectory independently, without any population-level coordination mechanism, thereby failing to capture the emergence of collective behaviors.

Prompt optimization Previous research on prompt optimization focuses on identifying an optimal prompt that enables an LLM to produce the best performance for a given class of tasks [5, 32, 36]. Existing methods can be categorized into three types. The first category focuses on how to select the optimal prompt given available candidates [11, 25]. For example, given a set of human-readable prompt candidates with unknown performance, ZOPO [11] embeds prompts into a continuous space and estimates update directions based on past performance, enabling efficient local exploration toward high-performing prompts. The second category considers both prompt refinement and optimal prompt selection, and addresses single-objective optimization [33, 38]. For example, Promptagent [33] enables an LLM to iteratively refine prompts based on observed errors, using MCTS to explore the space of prompt modifications. The third category considers both prompt refinement and prompt selection, with a focus on multi-objective optimization [12, 26, 27, 39, 41]. These works focus on balancing multiple objectives. For example, ParetoPrompt [41] uses a pre-trained language model as a policy, which is further optimized via reinforcement learning to achieve multi-objective prompt optimization.

Unlike prior work that focuses on finding a single prompt to achieve good performance on a specific task (single or multiple objectives), we aim to address a multi-prompt, multi-objective optimization problem. Specifically, our goal is to find an optimal set of prompts that jointly optimizes multiple objectives.

7 Conclusion

In this work, we design M2LSimu for LLM-based mobility simulation. It leverages mobility measures from shared data as guidance to adjust individual-level prompts in order to reproduce realistic

population-level mobility behavior. Our framework applies coarse-grained adjustment strategies guided by mobility measures, progressively enabling fine-grained individual-level adaptation while satisfying multiple population-level mobility objectives under a limited budget. Experiments show that M2LSimu significantly outperforms other LLM-based simulations.

References

- [1] Prabin Bhandari, Antonios Anastasopoulos, and Dieter Pfoser. 2024. Urban mobility assessment using llms. In *Proceedings of the 32nd ACM International Conference on Advances in Geographic Information Systems*. 67–79.
- [2] Nicolas Bougie and Narimawa Watanabe. 2025. Citysim: Modeling urban behaviors and city dynamics with large-scale llm-driven agent simulation. In *Proceedings of the 2025 Conference on Empirical Methods in Natural Language Processing: Industry Track*. 215–229.
- [3] Dirk Brockmann, Lars Hufnagel, and Theo Geisel. 2006. The scaling laws of human travel. *Nature* 439, 7075 (2006), 462–465.
- [4] U.S. Census Bureau. 2025. American Community Survey (ACS). <https://www.census.gov/programs-surveys/acs.html>.
- [5] Jiale Cheng, Xiao Liu, Kehan Zheng, Pei Ke, Hongning Wang, Yuxiao Dong, Jie Tang, and Minlie Huang. 2024. Black-box prompt optimization: Aligning large language models without model training. In *Proceedings of the 62nd Annual Meeting of the Association for Computational Linguistics (Volume 1: Long Papers)*. 3201–3219.
- [6] Yuwei Du, Jie Feng, Jian Yuan, and Yong Li. 2025. CAMS: A CityGPT-Powered Agentic Framework for Urban Human Mobility Simulation. *arXiv preprint arXiv:2506.13599* (2025).
- [7] Zipei Fan, Xuan Song, Yinghao Liu, Zhiwen Zhang, Chuang Yang, Quanjun Chen, Renhe Jiang, and Ryosuke Shibusaki. 2020. Human mobility based individual-level epidemic simulation platform. *SIGSPATIAL Special* 12, 1 (2020), 34–40.
- [8] Jie Feng, Zeyu Yang, Fengli Xu, Haisu Yu, Mudan Wang, and Yong Li. 2020. Learning to simulate human mobility. In *Proceedings of the 26th ACM SIGKDD international conference on knowledge discovery & data mining*. 3426–3433.
- [9] Haoyu Geng, Guanjie Zheng, Zhengqing Han, Hua Wei, and Zhenhui Li. 2022. HMES: A Scalable Human Mobility and Epidemic Simulation System with Fast Intervention Modeling. In *2022 IEEE Smartworld, Ubiquitous Intelligence & Computing, Scalable Computing & Communications, Digital Twin, Privacy Computing, Metaverse, Autonomous & Trusted Vehicles (SmartWorld/UIC/ScalCom/DigitalTwin/PriComp/Meta)*. IEEE, 468–475.
- [10] Marta C Gonzalez, Cesar A Hidalgo, and Albert-Laszlo Barabasi. 2008. Understanding individual human mobility patterns. *Nature* 453, 7196 (2008), 779–782.
- [11] Wenyang Hu, Yao Shu, Zongmin Yu, Zhaoxuan Wu, Xiaoliang Lin, Zhongxiang Dai, See-Kiong Ng, and Bryan Kian Hsiang Low. 2024. Localized zeroth-order prompt optimization. *Advances in Neural Information Processing Systems* 37 (2024), 86309–86345.
- [12] Yasaman Jafari, Dheeraj Mekala, Rose Yu, and Taylor Berg-Kirkpatrick. 2024. Morl-prompt: An empirical analysis of multi-objective reinforcement learning for discrete prompt optimization. *arXiv preprint arXiv:2402.11711* (2024).
- [13] WANG JIAWEI, Renhe Jiang, Chuang Yang, Zengqing Wu, Ryosuke Shibusaki, Noboru Koshizuka, Chuan Xiao, et al. 2024. Large language models as urban residents: An llm agent framework for personal mobility generation. *Advances in Neural Information Processing Systems* 37 (2024), 124547–124574.
- [14] Chenlu Ju, Jiaxin Liu, Shobhit Sinha, Hao Xue, and Flora Salim. 2025. Trajllm: A modular llm-enhanced agent-based framework for realistic human trajectory simulation. In *Companion Proceedings of the ACM on Web Conference 2025*. 2847–2850.
- [15] Pierre-Yves Lajoie, Bobak Hamed Baghi, Sachini Herath, Francois Hogan, Xue Liu, and Gregory Dudek. 2024. PEOPLEx: Pedestrian opportunistic positioning leveraging IMU, UWB, BLE and WiFi. In *ICC 2024-IEEE International Conference on Communications*. IEEE, 3518–3523.
- [16] Siyu Li, Toan Tran, Haowen Lin, John Krumm, Cyrus Shahabi, Lingyi Zhao, Khurram Shafique, and Li Xiong. 2024. Geo-llama: Leveraging llms for human mobility trajectory generation with spatiotemporal constraints. *arXiv preprint arXiv:2408.13918* (2024).
- [17] Yifan Liu, Xishun Liao, Haoxuan Ma, Brian Yueshuai He, Chris Stanford, and Jiaqi Ma. 2024. Human Mobility Modeling with Household Coordination Activities under Limited Information via Retrieval-Augmented LLMs. *arXiv preprint arXiv:2409.17495* (2024).
- [18] Xinyi Mou, Xuanwen Ding, Qi He, Liang Wang, Jingcong Liang, Xinnong Zhang, Libo Sun, Jiayu Lin, Jie Zhou, Xuanjing Huang, et al. 2024. From individual to society: A survey on social simulation driven by large language model-based agents. *arXiv preprint arXiv:2412.03563* (2024).
- [19] Farshid Nooshi and Suining He. 2025. Multi-Agent Reinforcement Learning for Dynamic Mobility Resource Allocation with Hierarchical Adaptive Grouping. *arXiv preprint arXiv:2507.20377* (2025).
- [20] U.S. Department of Transportation. 2022. 2022 National Household Travel Survey User's Guide. Nine-wave national household travel behavior survey since 1969; rich socio-demographic, trip mode/purpose data.
- [21] Kun Ouyang, Reza Shokri, David S Rosenblum, and Wenzhuo Yang. 2018. A non-parametric generative model for human trajectories. In *IJCAI*, Vol. 18. 3812–3817.
- [22] Jinghua Piao, Yuwei Yan, Jun Zhang, Nian Li, Junbo Yan, Xiaochong Lan, Zhihong Lu, Zhiheng Zheng, Jing Yi Wang, Di Zhou, et al. 2025. Agentsociety: Large-scale simulation of llm-driven generative agents advances understanding of human behaviors and society. *arXiv preprint arXiv:2502.08691* (2025).
- [23] Christian M Schneider, Vitaly Belik, Thomas Couronné, Zbigniew Smoreda, and Marta C González. 2013. Unravelling daily human mobility motifs. *Journal of The Royal Society Interface* 10, 84 (2013), 20130246.
- [24] Chenyang Shao, Fengli Xu, Bingbing Fan, Jingtao Ding, Yuan Yuan, Meng Wang, and Yong Li. 2024. Chain-of-planned-behaviour workflow elicits few-shot mobility generation in llms. *arXiv preprint arXiv:2402.09836* (2024).
- [25] Chengshuai Shi, Kun Yang, Zihan Chen, Jundong Li, Jing Yang, and Cong Shen. 2024. Efficient prompt optimization through the lens of best arm identification. *Advances in Neural Information Processing Systems* 37 (2024), 99646–99685.
- [26] Somanshu Singla, Zhen Wang, Tianyang Liu, Abdullah Ashfaq, Zhiting Hu, and Eric Xing. 2024. Dynamic rewarding with prompt optimization enables tuning-free self-alignment of language models. In *Proceedings of the 2024 Conference on Empirical Methods in Natural Language Processing*. 21889–21909.
- [27] Ankita Sinha, Wendi Cui, Kamalika Das, and Jiaxin Zhang. 2024. Survival of the Safest: Towards Secure Prompt Optimization through Interleaved Multi-Objective Evolution. *arXiv preprint arXiv:2410.09652* (2024).
- [28] Chaoming Song, Tal Koren, Pu Wang, and Albert-László Barabási. 2010. Modelling the scaling properties of human mobility. *Nature physics* 6, 10 (2010), 818–823.
- [29] Kaitao Song, Xu Tan, Tao Qin, Jianfeng Lu, and Tie-Yan Liu. 2020. Mpnet: Masked and permuted pre-training for language understanding. *Advances in neural information processing systems* 33 (2020), 16857–16867.
- [30] Heng Tan, Yukun Yuan, Shuxin Zhong, and Yu Yang. 2023. Joint rebalancing and charging for shared electric micromobility vehicles with energy-informed demand. In *Proceedings of the 32nd ACM International Conference on Information and Knowledge Management*. 2392–2401.
- [31] Eran Toch, Boaz Lerner, Eyal Ben-Zion, and Irad Ben-Gal. 2019. Analyzing large-scale human mobility data: a survey of machine learning methods and applications. *Knowledge and Information Systems* 58, 3 (2019), 501–523.
- [32] Prashant Trivedi, Souradip Chakraborty, Avinash Reddy, Vaneet Aggarwal, Amit Singh Bedi, and George K Atia. 2025. Align-pro: A principled approach to prompt optimization for llm alignment. In *Proceedings of the AAAI Conference on Artificial Intelligence*, Vol. 39. 27653–27661.
- [33] Xinyuan Wang, Chenxi Li, Zhen Wang, Fan Bai, Haotian Luo, Jiayou Zhang, Nebojsa Jojic, Eric P Xing, and Zhiting Hu. 2023. Promptagent: Strategic planning with language models enables expert-level prompt optimization. *arXiv preprint arXiv:2310.16427* (2023).
- [34] Wayne Wu, Honglin He, Jack He, Yiran Wang, Chenda Duan, Zhizheng Liu, Quanyi Li, and Bolei Zhou. 2024. Metaurban: An embodied ai simulation platform for urban micromobility. *arXiv preprint arXiv:2407.08725* (2024).
- [35] Wayne Wu, Honglin He, Chaoyuan Zhang, Jack He, Seth Z Zhao, Ran Gong, Quanyi Li, and Bolei Zhou. 2025. Towards autonomous micromobility through scalable urban simulation. In *Proceedings of the Computer Vision and Pattern Recognition Conference*. 27553–27563.
- [36] Yurong Wu, Yan Gao, Bin Benjamin Zhu, Zheneng Zhou, Xiaodi Sun, Sheng Yang, Jian-Guang Lou, Zhiming Ding, and Linjun Yang. 2024. Strago: Harnessing strategic guidance for prompt optimization. *arXiv preprint arXiv:2410.08601* (2024).
- [37] Takahiro Yabe, Kota Tsubouchi, Toru Shimizu, Yoshihide Sekimoto, Kaoru Sezaki, Esteban Moro, and Alex Pentland. 2024. YJMOb100K: City-scale and longitudinal dataset of anonymized human mobility trajectories. *Scientific Data* 11, 1 (2024), 397.
- [38] Sheng Yang, Yurong Wu, Yan Gao, Zheneng Zhou, Bin Benjamin Zhu, Xiaodi Sun, Jian-Guang Lou, Zhiming Ding, Anbang Hu, Yuan Fang, et al. 2024. Ampo: Automatic multi-branched prompt optimization. *arXiv preprint arXiv:2410.08696* (2024).
- [39] Haoqi Yuan, Yuhui Fu, Feiyang Xie, and Zongqing Lu. 2024. Pre-trained multi-goal transformers with prompt optimization for efficient online adaptation. *Advances in Neural Information Processing Systems* 37 (2024), 55086–55114.
- [40] Yuan Yuan, Yuheng Zhang, Jingtao Ding, and Yong Li. 2025. WorldMove, a global open data for human mobility. *arXiv preprint arXiv:2504.10506* (2025).
- [41] Guang Zhao, Byung-Jun Yoon, Gilchan Park, Shantenu Jha, Shinjae Yoo, and Xiaoning Qian. 2025. Pareto prompt optimization. In *The Thirteenth International Conference on Learning Representations*.
- [42] Yuanshao Zhu, Yongchao Ye, Shiyao Zhang, Xiangyu Zhao, and James Yu. 2023. Difftraj: Generating gps trajectory with diffusion probabilistic model. *Advances in Neural Information Processing Systems* 36 (2023), 65168–65188.

A Appendix

A.1 Supplementary analysis: preservation of human mobility scaling laws in coarse-grained data

In this section, we provide additional results that complement Section 2.3. Based on both real-world and coarse-grained data, we compare stay duration distributions and visitation frequency from temporal and spatial-temporal perspectives (Figures 9 and 10). We find that the distributions obtained from coarse-grained data closely match those obtained from the original real-world trajectories, indicating that coarse-graining preserves key scaling laws of mobility.

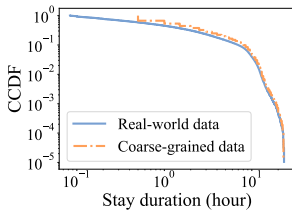


Figure 9: Stay duration distributions (Real vs. Coarse-grained).

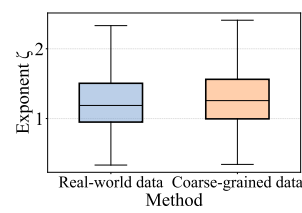


Figure 10: Visitation frequency (Real vs. Coarse-grained).

A.2 Effect of prompt adjustment

To assess whether mobility measures-guided prompt adjustment improves behavioral realism, we perform scaling-law analysis to compare real-world data with simulations before (M2LSimu w/o PA) and after adjustment (M2LSimu), considering both spatial and spatial-temporal aspects.

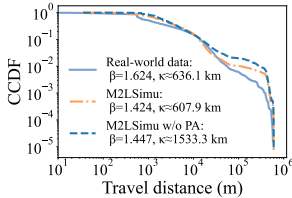


Figure 11: Effect of prompt adjustment on travel distance.

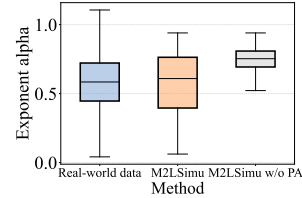


Figure 12: Effect of prompt adjustment on exploration.

Figure 11 shows the results for travel distance. For visualization clarity, travel distances are clipped to a predefined maximum threshold (i.e., 600km) during plotting only; all reported metrics are computed using the full dataset. We observe that, after adjustment, the travel distance distribution becomes closer to the real-world data. In addition, the cutoff values obtained from fitting the truncated power-law distribution are more consistent with those of the real data, better reflecting realistic human activity ranges.

Figure 12 presents the distribution of the exploration exponent α across all users. Before adjustment, both the distribution and the median value of the exploration exponent α differ from the real-world data, with higher values indicating overestimated exploration behavior and insufficient representation of population-level heterogeneity. After adjustment, the distribution becomes closer to that of the real-world data, indicating improved capture of population-level diversity. In particular, the median value of α aligns more

closely with the real-world data, consistent with findings reported in prior work.

A.3 M2LSimu optimization algorithm

Algorithm 1 M2LSimu optimization algorithm

```

1: Input: initial state  $s_0$ , action space  $\mathcal{A}$ , exploration constant  $c$  and  $c_g$ , maximum depth.
2: Initialize root node  $v_0$  with state  $s_0$ 
3: Initialize global statistics  $Q_g(a), N_g(a)$  for all  $a \in \mathcal{A}$ 
4: for  $i = 1$  to  $N_{iter}$  do
5:   if  $j = 1$  then ▷ Root warm-up
6:     for all  $a \in \mathcal{A}$  do
7:        $(r, s') \leftarrow \text{EVALUATE}(s_0, a)$ 
8:       Update  $Q_g(a), N_g(a)$ 
9:     end for
10:   end if
11:    $v \leftarrow v_0$ 
12:   Initialize empty trajectory  $\tau$  ▷ Selection
13:   while  $v$  has expanded children and  $v$  is not terminal do
14:      $a \leftarrow \arg \max_{a \in \text{Children}(v)} \text{UCT}(v, a)$ 
15:     Append  $(v.state, a)$  to  $\tau$ 
16:      $v \leftarrow \text{child}(v, a)$ 
17:   end while ▷ Expansion
18:   Construct candidate set  $C$  using global filtering
19:   for all  $a \in C$  do
20:      $(r_a, s_a) \leftarrow \text{EVALUATE}(v.state, a)$ 
21:   end for
22:    $a^* \leftarrow \arg \max_{a \in C} r_a$ 
23:   Create child node for  $s_{a^*}$ 
24:   Append  $(v.state, a^*)$  to  $\tau$ 
25:    $s_{\text{roll}} \leftarrow s_{a^*}$  ▷ Simulation
26:   for  $t = 1$  to  $L$  do
27:     if terminal condition satisfied at  $s_{\text{roll}}$  then
28:       break
29:     end if
30:     Construct candidate set  $C$  using global filtering
31:      $a \leftarrow \arg \max_{a \in C} r(s_{\text{roll}}, a)$ 
32:      $(r, s') \leftarrow \text{EVALUATE}(s_{\text{roll}}, a)$ 
33:     Append  $(s_{\text{roll}}, a)$  to  $\tau$ 
34:      $s_{\text{roll}} \leftarrow s'$ 
35:   end for ▷ Back-propagation
36:   Compute cumulative return  $G$  from trajectory  $\tau$ 
37:   Update  $Q(s, a)$  and visit counts for all  $(s, a) \in \tau$ 
38:   Update global statistics  $Q_g(a), N_g(a)$ 
39: end for
40: return root node  $v_0$ 

```

A.4 Prompt example

Action generation prompt example

ROLE

You are an expert in human mobility modeling, urban science, statistical physics of mobility, and LLM-based synthetic population simulation. Your expertise includes interpreting heavy-tailed spatial distributions and diagnosing behavioral biases in synthetic mobility data.

BACKGROUND

The simulated data is created by feeding human personas (profiles) into an LLM, which generates mobility trajectories. We compare real-world mobility data with simulated mobility data generated by an LLM. The objective is to improve simulation realism by adjusting persona design or constraining behavioral rules. The focus is on population-level behavioral interpretation rather than purely statistical comparison.

INPUT DATA

DEFINITIONS

- Radius of gyration = spatial extent of individual mobility.
- Radius reflects overall activity space and movement scale of individuals rather than single-step movement.
- Statistical differences should be interpreted as indicators of differences in population mobility lifestyles.

ANALYSIS GOALS

- Population composition biases
- Missing or exaggerated activity-space archetypes
- Behavioral causes of distribution mismatch
- Ways to adjust personas or behavioral rules

TASK REQUIREMENTS

TASK 1 – Population-level Diagnosis

From a human mobility perspective, briefly explain what the observed differences suggest about overall activity space. Describe whether the simulated population tends to move within larger or smaller areas than real people, and identify which general mobility archetypes may be overrepresented or underrepresented.

Keep explanations concise and behavior-focused; avoid detailed mathematical discussion.

TASK 2 – Population Group

Goal: Define a practical radius-based segmentation schema.
Requirements:

- Define 4–6 radius groups that partition individuals by activity-space size (small → large).
- Groups must be defined by radius magnitude.
- For each group provide: Group name, Radius range (clear thresholds or relative scale), One-sentence

behavioral description and Target proportion (%) representing a realistic population distribution

- Keep output concise and structured.

TASK 3 – Adjustment Strategy

For each group defined in Task 2, provide concrete and implementable adjustments aimed at improving simulation realism.

Examples include:

- Adding behavioral constraints (e.g., stronger home-/work anchors)
- Reducing excessive spatial dispersion
- Increasing routine or location stability
- Adjusting exploration probability
- Adding socio-demographic diversity constraints

Adjustments must be actionable for LLM-based persona generation pipelines.

OUTPUT FORMAT

- (1) Population Diagnosis
- (2) Population Groups Table
 - Columns:
 - Group Name | Radius Range | Behavioral Description | Target proportion
- (3) Adjustment Strategy (group-by-group structured suggestions)